Theoretical Study of 8-hydroxyquinoline Derivatives as Potential Antennas in Lanthanide complexes: Photophysical Properties and Elucidation of Energy Transfer Pathways.

Juan Julián Santoyo-Flores[1], Dayán Páez-Hernández[2]

[1]Doctorado en Fisicoquímica Molecular, Universidad Andres Bello, República 275, Santiago, Chile.

julian.qtpgd@gmail.com

[2]Center of Applied Nanoscience (CANS), Universidad Andres Bello, Republica 275, Santiago, Chile.

dayan.paez@unab.cl

August 31, 2021

Abstract

A series of 8-hydroxyquinoline derivatives were characterized and tested as potential antennas in a set of designed lanthanide complexes. The molecular structure and ligand localized nature of the excited states were studied in the framework of the multiconfigurational methods CASSCF/NEVPT2 combined with TD-DFT-based approaches, which allows applying a fragmentation scheme in the analysis of the most probable sensitization pathway via antenna effect. The photophysical properties of all the complexes and antennas were carefully analyzed, and the most probable energy transfer pathways were elucidated. Rate constants for photophysical processes involved in the mechanism were calculated, showing a significant contribution of the vibronic coupling in all cases and the predominant intersystem-crossing between S_1 and T_1 states was demonstrated from the analysis of the nature of the wave function of those states. The energy transfer process described herein demonstrates the possibility of Eu(III) and Nd(III) sensitization by the studied ligands. The proposed methodology gives a complete picture of the antenna excited state dynamics.

1 Introduction

In recent years, the use of lanthanide complexes as luminescent materials has opened an important area of technological[1, 2] and medical development[3, 4]. These materials have a wide range of applications in displays[5], biomedical dyes[6], lasers[7], LEDs[8], and different studies demonstrate its potential use in photodynamic therapy (PDT)[9]. Lanthanides have attracted interest because of their unique spectroscopic properties associated with the inner character of the 4f shell due to the shielding by the 5s and 5p shells.

Thus, the effect of the ligand field is not significantly over the 4f shell. On the other hand, the effects of the spin-orbit coupling and the scalar relativistic effects, both direct and indirect, are important due to the heavy atom effect. In consequence, the lanthanide complexes exhibit narrow emission bands well-defined in a wide spectral range, long excited states lifetimes, and stable 3+ oxidation states for the ions[10]. The electronic transitions f-f in the 4f shell are forbidden by the Laporte rule[11, 12]. Therefore, the absorption coefficients are low, and the direct excitation of the lanthanide ion (represented in this work as Ln(III)) is inefficient. To obtain an efficient sensitization of the Ln(III), the antenna effect, emerges as an effective process to sensitize the lanthanide ion[13, 14]. This action occurs through energy transfer from the excited level of the antenna to the resonant level of the Ln(III).

The selection of the antenna is essential to obtain highly luminescent lanthanide complexes[15, 16]. In this context, a good organic antenna should generate photoinduced $^3(n \rightarrow \pi^*)$ and $^3(\pi \rightarrow \pi^*)$ states, possess a rigid structure and it is able to saturate the coordination sphere. On the other hand, and during the last few decades, the research focus for the biological applications of lanthanide complexes has been placed on one special target: DNA base pair mismatches. Mismatches normally arise during cell proliferation as a result of errors in the DNA replication process, although they are usually corrected by the mismatch repair mechanism. However, mismatches are remarkably more abundant in aging cells, cells with high proliferation rates (e.g. infected with certain viruses) or in cells exposed to mutagenic agents. Therefore, complexes with a high binding affinity to DNA, specially intercalation in the base pairs affected by mismatch represent potential candidates to develop new drugs able to selectively detect damage cells and for PDT treatment[17, 18, 19]. In the view of the above, bio-inspired ligands as alkaloids, flavonoids, carotenoids[20, 21, 22], but, in special the derivatives of 8-hydroxyquinoline[23, 24, 25], as the clioquinol (5-chloro-7-iodo-quinolin-8-ol) (ClIQH), have characteristics to be consider as potential antenna. Some of this characteristics, are the capacity to absorb radiation in the UV/Vis region, rigid structure, and the heavy atom effect. This ligand exhibits high binding affinity to DNA[26, 27, 28], being the intercalation the possible binding mechanism[29, 30]. In the present work, we propose a systematic *ab initio* study to evaluate the capacity of a series of 8-hydroxyquiinolines derivatives (See Scheme 1) as potential antennas. Accordingly, we designed a series of lanthanide complex models based on previous experimental reports[23, 25, 37]. The purpose has been to elucidate the most probable energy transfer pathways in these lanthanide complexes with the following design $[Ln(XYQ)_4]^-$ where the Ln= Eu, Nd, Tb.

Quantum chemistry provides reliable tools to estimate the energy of the electronic states in these type of molecules[31]. The systems under study require considering the effect of the delocalized charge distribution in the antenna and its impact on the energetic position of its first triplet state. This state is involved in the energy transfer mechanism to the Ln(III). Moreover, the multireference character of the wave function of the metal states due to the large number of low-lying configurations resulting from the f^n shell of the Ln(III) must be considered[32]. In this context, the multireference *ab initio* methods can be used to estimate, with precision, the photophysics in lanthanide complexes including the quasi-degeneration of the 4f-shell and its consequences. This methodology allows, also, the inclusion of the relativistic effects essential in this type of

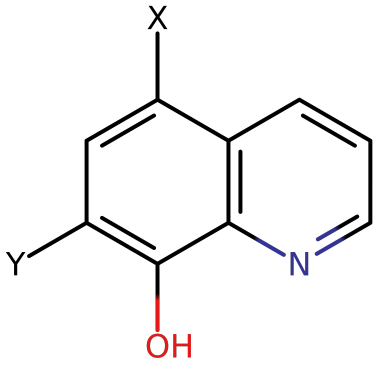

1) X=Cl, Y=H
2) X=Cl, Y=Br
3) X=Cl, Y=Cl
4) X=Cl, Y=I

Scheme 1: **1**)5-chloro-quinolin-8-ol. **2**)7-bromo-5-chloro-quinolin-8-ol. **3**)5,7-dichloro-quinolin-8-ol. **4**)5-chloro-7-iodo-quinolin-8-ol

system.[33, 34]. The complete active space self-consistent field (CASSCF) method, in combination with the second-order perturbation theory NEVPT2 method, arose as a reliable procedure for the study of lanthanide complexes. However, this level of theory is expensive; therefore, Beltran-Leiva *et. al.*[35, 36], proposed a fragmentation scheme, where the antenna and the lanthanide fragments are calculated separately but at the same level of theory for the acquisition of the ground and excited states in both fragments. In the next section the details of the calculations are presented followed by the presentation and discusion of the main results obtained in this work.

2 Computational Details

All the structures of the complexes were optimized using the Amsterdam Density Functional (ADF) Package[38]. The zeroth-order regular approximation (ZORA)[39, 40] Hamiltonian of two-components was used to include the scalar relativistic effects. Generalized gradient approximation exchange-correlation functional BP86 along with the standard Slater-type orbital (STO) with quality of triple-ζ double plus polarization function (TZ2P) basis set [41, 42, 43] was used for all the atoms. Frequencies were calculated to verify that the obtained structures are minimums. Frequency calculations were also performed in ORCA 4.2.1 code[44] for the ligands obtained as fragments of the complex system. The Hessian matrices obtained in these calculations, for the ground and first excited (optimized) singlets (S_0 and S_1) were collected and used to study the excited states dynamic using the ORCA_ESD module, which estimates the fluorescence, inter-system crossing (ISC), and phosphorescence rates via the vibrational coupling between electronic states. Spin-orbit coupling was introduced via spin-orbit mean-field approximation (SOMF)[45, 46] considering a sufficiently large amount of states that allow a god mixing between them. For excited singlets states used in these calculations, TD-DFT

optimizations were carried out using the restricted KS determinant as the reference. In contrast, the triplet states were optimized using normal unrestricted KS ground-state calculations with a spin polarization of 2. To accelerate the computation of two-electron integrals, the resolution of identity approximation was used for the Coulomb part (RIJ), and the chain of spheres algorithm for the exchange part (COSX)[47, 48], with the corresponding auxiliary basis and grid settings. The DFT grid was set to GRID5, and the COSX grid was set to GRIDX5.

The first step in the determination of the most probable sensitization pathway via the antenna effect was the absorption spectra that were assigned in the framework of the scalar relativistic time-dependent Density Functional Theory (SR-TDDFT) in combination with the Coulomb-attenuated hybrid exchange-correlation functional (CAM-B3LYP)[49]. The calculations were done for the whole complexes, and the ligands were obtained as fragments, in the same way explained above. These calculations were performed to show that the absorption spectra of the complexes are ligand centered with the aim to apply, *a posteriori*, the fragmentation scheme proposed by Beltrán-Leiva *et. al.*[35, 36]. Muticonfigurational calculations were performed to correctly reproduce the effect of static correlation as a consequence of the many low-lying states associated with the $4f^n$ configurations. Complete Active Space Self Consistent Field (CASSCF)[50, 51] was used, followed by N-electron Valence Perturbation Theory method (NEVPT2)[52] to include both static and dynamic correlation. Spin-orbit coupling was introduced in the second step via Quasi-Degenerate Perturbation Theory approximation (QDPT)[45, 46]. For lanthanide, the minimal active space was considered, CAS(n,7) where n=3, 6, 8 for Nd, Eu, and Tb, respectively, because of the well-known core-like character of the 4f-shell electrons and the little metal-ligand interaction. Ligands were treated exactly at the same level of theory regarding an active space of eight electrons in eight orbitals CAS(8,8) carefully selected from the analysis of the absorption spectra obtained at the TDDFT level. The resulting states were used to establish the most probable sensitization pathway mechanism by applying the Reinhoudt and Latva rules for inter-system crossing (ISC) and energy transfer (ET), respectively[66, 69]. At this point it is important to clarify that the Reinhoudt rule for the ISC rate represents a guideline in terms of the energy difference for higher ISC efficiency and does not necessarily establish that this mechanism occurs between S_1 and T_1. El-Sayed rule states that SOC is larger for the states of different orbital character (both spin and orbital moment are changed in the transition)[53, 54]. Therefore, if both T_1 and S_1 are dominated by the same orbitals, and the gap is 3000-5000cm^{-1}, ISC(S_1-T_1) should be small. It means that some other triplets quasidegenerate with S_1 should be involved for an efficient ISC[55, 56], this exploration was performed in this work and is included in the discussion below. Scalar relativistic effects were included via Douglas-Kroll-Hess Hamiltonian[57], and scalar relativistically re-contracted SARC2-DKH-QZV basis set was used for lanthanide atom[58] while def2-TZVP[59, 60] was used for the atoms except I which was treated with def2-SVP[61] and SDD pseudopotential.

3 Results and Discussion

The theoretical protocol used in this work to elucidate the most probable energy transfer process due to antenna effect in lanthanide complexes is based on the premise that the absorption spectra of the complexes are due to the antenna ligand. In consequence, the emission of the Ln(III) is promoted by the antenna excited state that transfers energy to the emissive state of Ln(III). This makes possible the characteristic emission bands for the different Ln(III). In this context, the methodology discussed above was applied to calculate the electronic levels of the antenna and the lanthanide fragments. The results of this work are presented as follows: First, the spectroscopic properties of the antennas are analyzed. Second, the excited state dynamics and the nature of the active orbitals of the ligands are presented. Third, the energy levels of the lanthanide are discussed to propose energy transfer mechanisms responsible for the complex emission.

3.1 Spectroscopic Properties of the Antenna.

Twelve complexes of the form $[Ln(HClQ)_4]^-$, $[Ln(BrClQ)_4]^-$, $[Ln(ClClQ)_4]^-$ and $[Ln(ClIQ)_4]^-$, where Ln = Eu, Tb, Nd were optimized and theoretically characterized in this work. The UV-Vis absorption spectra were calculated for the complexes and the antenna fragments obtained from the optimized structures. The group of $[Ln(HClQ)_4]^-$, $[Ln(BrClQ)_4]^-$, $[Ln(ClClQ)_4]^-$ complexes show two absorption bands among 280-420 nm corresponding to a $\pi \rightarrow \pi^*$ transition ligand centered and slightly blue-shifted when comparing with the free ligand, see Figure 1 a). In the analyzed region no $n \rightarrow \pi^*$ transitions were found for the free ligands and due to coordination, these bands are not expected or would be low in intensity in the complexes. The obtained spectra are in agreement with the experimental reports in similar cases.[62, 63]. The $[Ln(ClIQ)_4]^-$ complex was analyzed in a separated form because present some interesting differences respect to the previous ones. As can be seen in Figure 1 b) the calculations allows to differentiate three different bands among 350-550 nm being the most intense a $\pi \rightarrow \pi^*$ transition between 350-400 nm followed by two less intense bands corresponding to a $n \rightarrow \pi^*$ transitions with high contribution of iodine substituent. As is shown in Figure 1, there are no significant differences between the absorption spectra of ligand and complexes and the position of the bands and its assignment are in agreement with previous reports. The electronic transitions assignment, presented in Table 1, corroborates that the transitions are ligand centered in this case and all other complexes (See the Electronic Supporting Information). This analysis of the absorption spectra allows to apply the fragmentation scheme discussed above in the following part of the work.

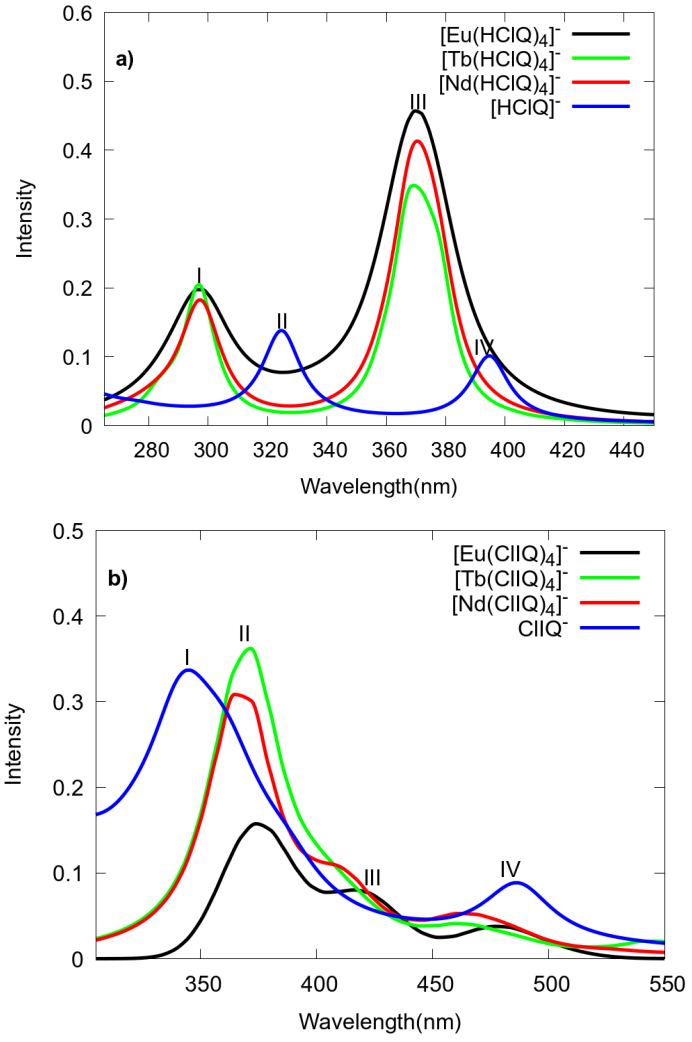

Figure 1: Calculated absorption spectra at SR-TDDFT level theory for the complexes a)$[Ln(HClQ)_4]^-$, b)$[Ln(ClIQ)_4]^-$ where Ln= Eu, Nd, Tb, and the antenna fragment from the optimized lanthanide complexes.

Table 1: Assignment of electronic transitions involved in the complexes and antennas with the design $[Ln(ClIQ)_4]^-$ using SR-TDDFT level theory.

Band	λ(nm)	f	Transition	Assignment
I	343	0.194	HOMO-1 → LUMO+1	$\pi \rightarrow \pi^*$ $[ClIQ]^-$
II	376	0.049	HOMO-2 → LUMO+3	$n \rightarrow \pi^*$ $[Eu(ClIQ)_4]^-$(*ligand centered*)
			HOMO-6 → LUMO	$\pi \rightarrow \pi^*$ $[Eu(ClIQ)_4]^-$ (*ligand centered*)
	371	0.098	HOMO-6 → LUMO	$\pi \rightarrow \pi^*$ $[Tb(ClIQ)_4]^-$ (*ligand centered*)
	366	0.059	HOMO-7 → LUMO+2	$\pi \rightarrow \pi^*$ $[Nd(ClIQ)_4]^-$ (*ligand centered*)
III	426	0.021	HOMO-1 → LUMO+2	$n \rightarrow \pi^*$ $[Eu(ClIQ)_4]^-$ (*ligand centered*)
			HOMO → LUMO+2	$n \rightarrow \pi^*$ $[Eu(ClIQ)_4]^-$ (*ligand centered*)
	413	0.017	HOMO-2 → LUMO+1	$n \rightarrow \pi^*$ $[Nd(ClIQ)_4]^-$ (*ligand centered*)
IV	485	0.009	HOMO-2 → LUMO+2	$n \rightarrow \pi^*$ $[Eu(ClIQ)_4]^-$ (*ligand centered*)
			HOMO-2 → LUMO	$n \rightarrow (\pi^*)$ $[Eu(ClIQ)_4]^-$ (*ligand centered*)
	461	0.012	HOMO-2 → LUMO	$n \rightarrow \pi^*$ $[Tb(ClIQ)_4]^-$ (*ligand centered*)
	457	0.008	HOMO-6 → LUMO	$n \rightarrow \pi^*$ $[Nd(ClIQ)_4]^-$ (*ligand centered*)
	487	0.066	HOMO → LUMO+5	$n \rightarrow \pi^*$ $[ClIQ]^-$

Because of the above, a possible sensitization process between the antenna and the Ln(III) is suggested. For the elucidation of the energy transfer pathways, the calculation of the electronic levels of the antennas as a result of the fragmentation scheme is necessary. The most probable sensitization pathway via antenna effect generally accepted involves antenna absorption. Following by the intersystem crossing (ISC) between the first excited singlet and the first triplet state, and finally, an energy transfer from the triplet state to the emissive state of lanthanide. To get more insight into this mechanism, a detailed analysis of the excited state dynamic was performed for all the proposed ligands. This study was performed using the approach proposed by Izsák *et. al.*[64] in 2018, where the rate for the transition between two states is determined from time-dependent perturbation theory, including vibronic coupling, using the so-called Fermi golden rule. The adiabatic hessian (AH) approximation was used in all cases, and the fraction of the rate due to the Herzberg-Teller effect was also included[65]. This level of theory required additional geometry optimization of the first excited singlet and triplet states. For the ISC and phosphorescence mechanisms, the spin-orbit coupling between the first thirty excited singlet and triplet states was included in the TDDFT calculations. In the Scheme 2 the calculated values for the rate constants of the fluorescence, phosphorescence, and intersystem crossing are presented. As it is possible to appreciate, the fluorescence rate in four ligands is in the range generally reported for this mechanism. Moreover, except in $[HClQ]^-$ the ISC mechanism has a rate one order of magnitude above the fluorescence rate, meaning that the population of the first excited triplet states is guaranteed in these ligands.

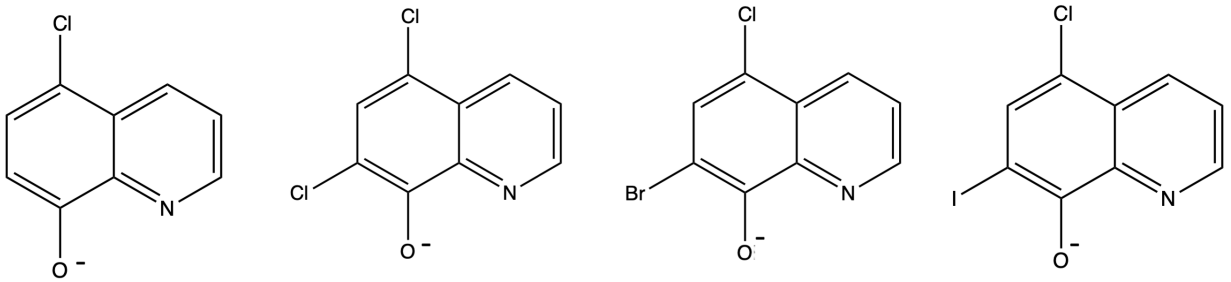

Scheme 2: Rate constants obtained for the free antenna fragments.

A more detailed analysis of the excited states electronic structure based on multiconfigurational calculations where an active space of eight electron in eight orbitals CAS(8,8) was considered show, in agreement with TDDFT calculations, that the first excited singlet state S_1 has a $n \rightarrow \pi^*$ character, meaning that, according to El-Sayed rule, that $^1(n \rightarrow \pi^*) \rightarrow {}^3(\pi \rightarrow \pi^*)$ will be faster than $^1(n \rightarrow \pi^*) \rightarrow {}^3(n \rightarrow \pi^*)$. From the analysis of the low lying triplets states electronic configurations presented in Scheme 3, it is easy

to see that in the four studied ligands the most probable and faster radiation-less ISC transition will occur to the first excited triplet T_1 which is, in all cases energetically below the the first excited singlet and has a $\pi \rightarrow \pi^*$ configuration (See Supplementary Information). The rest of the excited triplets around the first excited singlet are of the same configuration (forbidden or slow ISC) or have a large energy difference to S_1 to be relevant in the ISC mechanism. It is well known that the El-Sayed forbidden ISC can be accelerated by the vibronic interaction between the involved states, however, the exploratory calculations do not reveals relevant contributions from the triplet states different to T_1 even including the Herzberg-Teller effects.

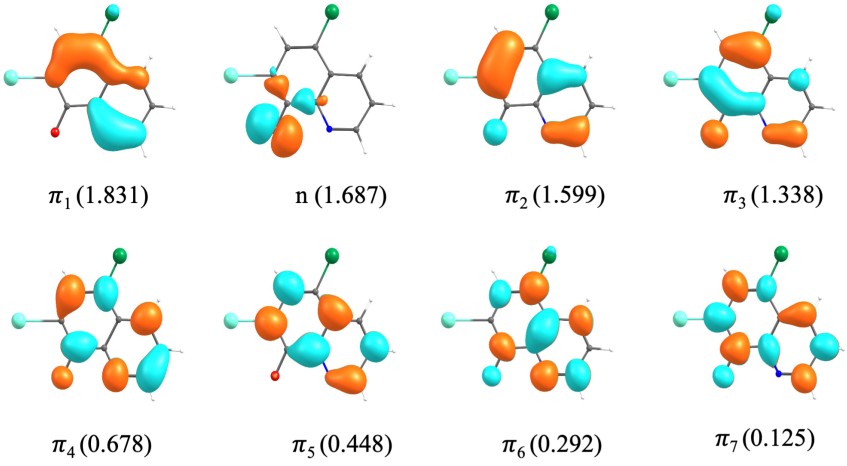

S_0 88% | $\pi_1^2\pi_2^2n^2\pi_3^2$ |

S_1 80% | $\pi_1^2\pi_2^2n^1\pi_3^2\pi_4^1$ | $(n \rightarrow \pi^*)$

T_1 75% | $\pi_1^2\pi_2^2n^2\pi_3^1\pi_4^1$ | +10% | $\pi_1^2\pi_2^2n^2\pi_3^1\pi_5^1$ | $(\pi \rightarrow \pi^*)$

T_2 81% | $\pi_1^2\pi_2^2n^1\pi_3^2\pi_4^1$ | $(n \rightarrow \pi^*)$

T_3 68% | $\pi_1^2\pi_2^2n^2\pi_3^1\pi_5^1$ | +12% | $\pi_1^2\pi_2^2n^2\pi_3^1\pi_4^1$ | $(\pi \rightarrow \pi^*)$

Scheme 3: Active orbitals and occupation numbers obtained for antenna fragment $[ClIQ]^-$ at CASSCF(8,8) level of theory.

Additionally, the heavy atom effect reinforces this mechanism. DFT calculations showed that the S_1-T_1 energy difference is in the range usually accepted by the Reinhoudt rule[66] to get the most efficient ISC mechanism. The vibronic coupling plays a central role in the matrix element of the electronic transition dipole calculated in each rate contributing in all cases with more than 90% of the final value. On the other hand, the calculated phosphorescence rates indicate a long lifetime of the excited triplet state. This state is relevant in the energy transfer mechanism. However, when Latva rules are not entirely fulfilled, it is possible the ligand emission. Two conclusions can be reached from these calculations regarding the suitability of these ligands as possible luminescence-sensitizing antennas in lanthanide ions. First, they have an efficient ISC with a consequent population of the first excited triplet state. Second, the lifetime of the excited triplet state

is sufficiently large to favors an energy transfer mechanism. Considering that the energy transfer mechanism in complexes with similar ligands has been reported in the range, 10^7-10^{10}s^{-1}[67, 68]. We conclude that if the Latva rule[69] is accomplished, these ligands can act as efficient antennas.

The next step in evaluating the most probable sensitization pathway was the calculation of the energetic position of the excited states from multiconfigurational calculations. In Table 2, the first four singlet and triplet states obtained at CAS(8,8)SCF/NEVPT2 level of theory are presented. The obtained values are in good correspondence with those reported in the literature[70]. As it is possible to appreciate, this level of calculation predicts energy differences between S_1-T_1 slightly below the values obtained at the DFT level. The $HClQ^-$ and $BrClQ^-$ cases were the best energy gap in the Reinhoudt rule sense. Nevertheless, the ISC is guaranteed in all cases.

Table 2: Calculated electronic levels for molecular antennas. All values are in cm^{-1}.

State	$[HClQ]^-$	$[ClClQ]^-$	$[ClIQ]^-$	$[BrClQ]^-$
T_1	19313.4	18154.6	19979.2	18582.9
T_2	25468.4	23130.2	23804.5	23978.4
T_3	27804.8	29778.4	28738.5	30425.3
T_4	32966.9	32543.8	34246.1	34443.6
S_1	24327.8	21689.7	23693.4	22964.6
S_2	28299.9	26187.9	28506.0	26872.6
S_3	29283.2	30388.3	29314.6	30996.2
S_4	34513.1	35613.3	34547.1	35392.2
$\Delta E_{S_1-T_1}$(DFT)	5308.0	5112.0	5121.0	5121.0
$\Delta E_{S_1-T_1}$(NEVPT2)	5014.4	3535.1	3714.2	4381.7

3.2 Electronic states of the lanthanide complexes and sensitization pathway

For treating lanthanide fragments obtained from the application of the fragmentation scheme, it is possible a reliable estimation of the electronic levels for Eu(III), Nd(III), and Tb(III) fragments. SO-CASSCF/NEVPT2 calculations were performed to determine the electronic levels of the lanthanide fragments considering the complete coordination sphere. The minimal active space was chosen for the three ions studied in this work, meaning 6, 3, and 8 electrons in seven 4f orbitals for Eu, Nd, and Tb, respectively. From CASSCF the representative wave functions for all the possible multiplicities associated with each electronic configuration are obtained and their energies corrected at second-order perturbation theory (NEVPT2). The spin-orbit coupling is introduced in a second step via QDPT. This methodology has been applied with success, previously showing good performance assigning the most probable sensitization pathway[35, 36, 32]. The calculations show that the emissive state for Eu(III):$^5D_0$ is at 18109.3 cm^{-1}, for Tb(III): $^5D_4$ at 22368.4 cm^{-1} and for Nd(III): $^4F_{3/2}$ at 12895.2 cm^{-1}, these calculated values are in good agreement with the reported in the literature[36, 71]. Besides, the most important transition bands are presented in Table 3; these values are accurately predicted with this methodology and in accordance with the experimental values[32, 72].

Table 3: Calculated emission lines for $[Ln(ClIQ)_4]^-$. All values are in nm.

$[Eu(ClIQ)_4]^-$	$[Nd(ClIQ)_4]^-$	$[Tb(ClIQ)_4]^-$
552.2($^5D_0 \rightarrow {}^7F_0$)	804.2($^4F_{3/2} \rightarrow {}^4I_{9/2}$)	615.0($^5D_4 \rightarrow {}^7F_0$)
569.2-560.1($^5D_0 \rightarrow {}^7F_1$)	944.1-934.8($^4F_{3/2} \rightarrow {}^4I_{11/2}$)	612.3-608.5($^5D_4 \rightarrow {}^7F_1$)
593.2-584.4($^5D_0 \rightarrow {}^7F_2$)	1177.8-1157.1($^4F_{3/2} \rightarrow {}^4I_{13/2}$)	596.2-589.7($^5D_4 \rightarrow {}^7F_2$)
619.0-622.5($^5D_0 \rightarrow {}^7F_3$)	1612.7-1516.9($^4F_{3/2} \rightarrow {}^4I_{15/2}$)	571.5-571.6($^5D_4 \rightarrow {}^7F_3$)
668.1-654.8($^5D_0 \rightarrow {}^7F_4$)		547.1-539.2($^5D_4 \rightarrow {}^7F_4$)
724.1-707.5($^5D_0 \rightarrow {}^7F_5$)		508.6-468.3($^5D_4 \rightarrow {}^7F_5$)
795.5-766.7($^5D_0 \rightarrow {}^7F_6$)		464.6-447.0($^5D_4 \rightarrow {}^7F_6$)

The energy transfer pathway in the lanthanide complexes usually occurs through the route $^1S^* \rightarrow^3 T^* \rightarrow Ln^*$. In this context, some rules are established for the efficient sensitization of the lanthanide ion. The first consideration is to guarantee the intersystem crossing (ISC) mechanism, where the difference in energy between the $S_1 - T_1$ states of the antenna is around ≈3000-5000cm^{-1} (discussed above for each ligand). The second rule is established for efficient energy transfer from the triplet state of the antenna to the emitting state of the Ln(III). The optimal gap is in the range of ≈ 2500–4000 cm^{-1}. Therefore, the elucidation of the most probable sensitization and emission pathways can be assigned from these rules. The Figure 2 and 3 show the energetic balance of the sensitization mechanism summarized as a Jablonski diagram. The energy gap between the emissive states of the lanthanide and all the antennas is shown in Table 4. As it is possible to see, the typical route of sensitization cannot be considered for Tb(III) complexes because their emissive state $^5D_4$ are above all the T_1 states from the different antennas. In consequence, the energy transfer process is not possible from this state. For Eu(III), the energy gap between the emissive state $^5D_0$ and the T_1 states

for all antennas is too close, activating the thermally competitive back energy transfer (BET). Consequently, a re-population of the excited triplet and the possible phosphorescent emission of the antenna. However, a more detailed analysis of the electronic states of the antenna ligands reveals that particularly $[ClClQ]^-$ ($3558cm^{-1}$) and $[BrClQ]^-$ ($4856cm^{-1}$) can transfer energy to the emissive state of the Eu(III) from their first excited singlet state. As discussed above, for these ligands, the S_1-T_1 energy difference calculated at the NEVPT2 level of theory was in the limits for an efficient ISC. In this context, an alternative sensitization pathway is completely plausible. At this point, it is necessary to take into account that, in general, the probability of energy transfer from a singlet state is small ($k_{ET} \approx 10^{-3}$-$10^5 s^{-1}$)[67, 68] and ISC, in this case, represents a source of significant competition resulting in poor sensitization from this route. In Tb(III), the gaps for the first excited singlet are insufficient to propose a similar pathway. For Nd(III), the gap between its emissive state $^4F_{3/2}$ and the antenna triplets is exceeded by an average of ≈ 2000 cm^{-1} of the ideal maximum value. Nevertheless, based on the literature, the sensitization in this will not be in the most efficient range, but is possible[73, 74].

Table 4: Calculated energy gap $T_1^* - Ln^*$ for all the complexes. All values are in cm^{-1}.

$\Delta E_{T_1^* - Ln^*}$				
Ln	$[HClQ]^-$	$[ClClQ]^-$	$[ClIQ]^-$	$[BrClQ]^-$
Eu($^5D_0$)	1204.1	45.3	1869.9	473.6
Tb($^5D_4$)	-3055.1	-4213.5	-2389.3	-3785.6
Nd($^4F_{3/2}$)	6418.2	5259.4	7084.0	5687.7

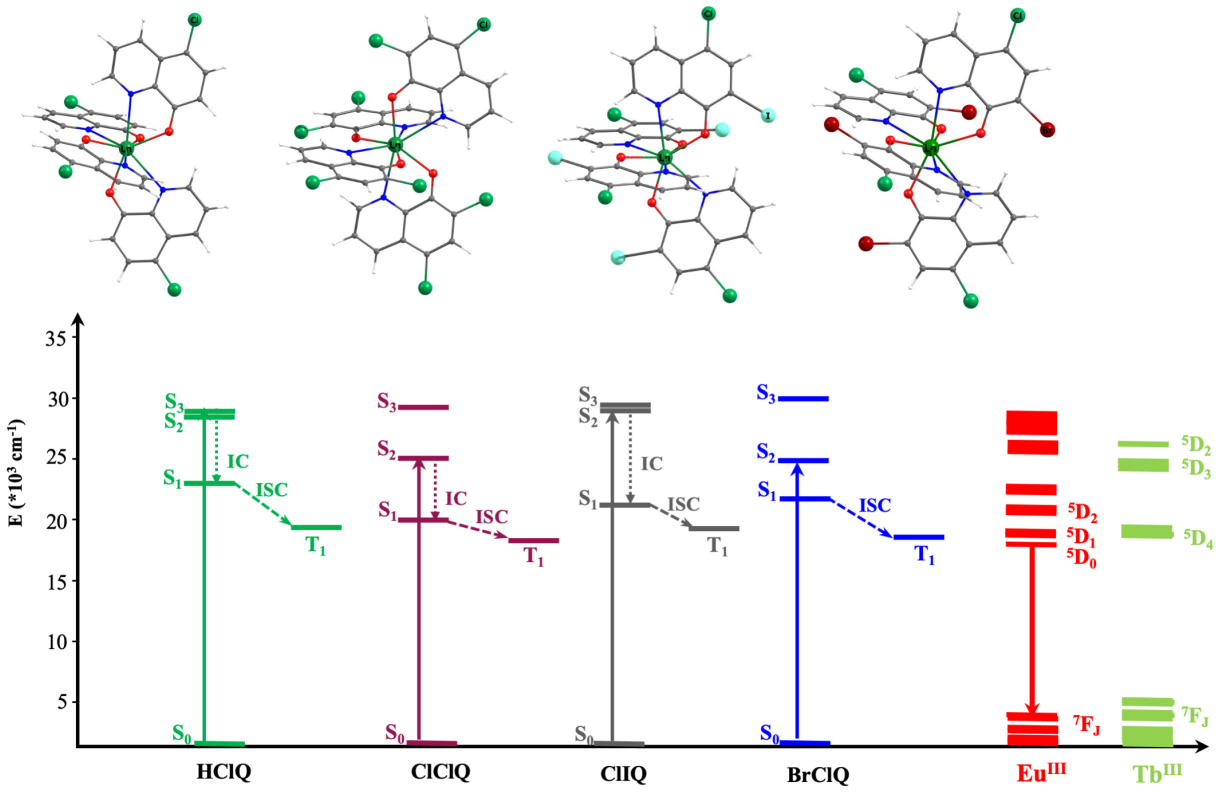

Figure 2: Most probable energy transfer pathways for $[Ln(XYQ)_4]^-$, where Ln= Tb, Eu. All the studied antennas were represented in the diagram for a potential sensitization pathway. All the energy states were calculated at the NEVPT2 level of theory.

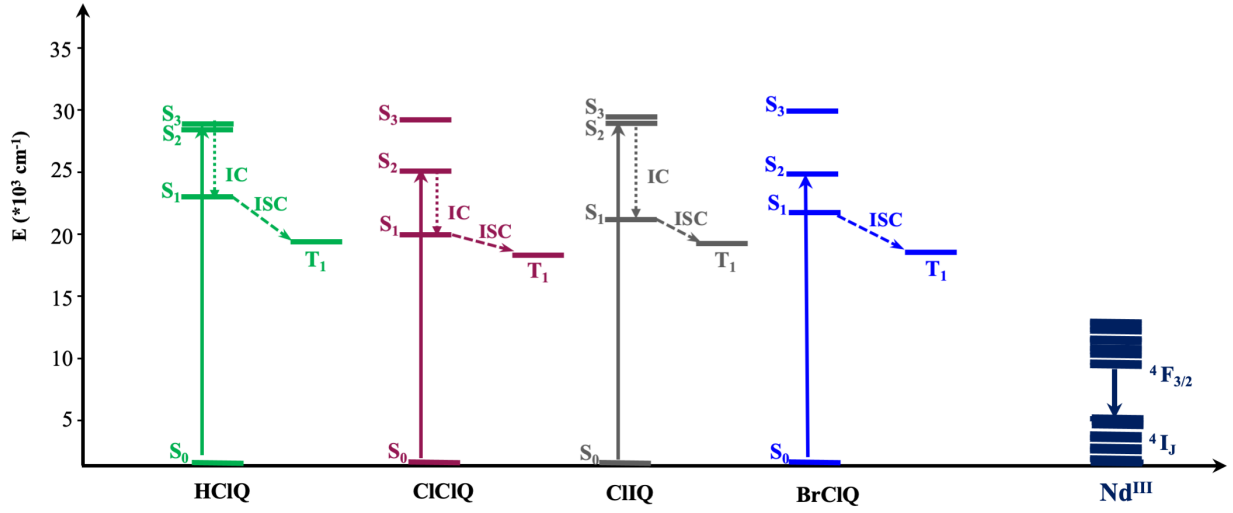

Figure 3: Most probable energy transfer pathways for $[Nd(XYQ)_4]^-$. All the studied antennas were represented in the diagram for a potential sensitization pathway. All the energy states were calculated at the NEVPT2 level of theory.

4 Conclusions

In this work, we presented a series of calculations to describe the capacity of a set of ligands to sensitize the emission in lanthanide complexes. The fragmentation scheme has been applied with success to describe the photophysical properties and excited-state dynamics of the antennas and lanthanide complexes. The excited-state dynamics of the antennas show that the vibronic coupling is the principal contribution to the final value of the rate constants involved in the sensitization pathway. The ISC is efficient in all antennas tested, making these antennas potential sensitizers. The CASSCF/NEVPT2 multiconfigurational methods along with TD-DFT methods allow to obtain a detailed description of the electronic structure. The elucidation of the energy transfer pathway of these antennas to sensitize a lanthanide ion as Nd(III) was possible, which is relevant considering that it is a difficult task for organic ligands. This work opens up the possibility to redesign an antenna as 8-hydroxyquinoline to sensitize lanthanide ions efficiently in combination with successfully tested and proven methodologies to describe the electronic structure of the lanthanide complexes as used in this work. Usually, the energy transfer pathway should include structural relaxation of the antenna ligand in its excited states, included in this work in the analysis of the excited states dynamics for both, first excited singlet (S_1) and triplet (T_1). This relaxation is a fast process; it proceeds in a femtosecond scale, and the structural changes can be relevant, thus leading to substantial changes in the excited state energies. In this work, however, the rigid structure of the ligands does not show significant changes in the studied excited states. This result is in favor of the accuracy of the predictions made in this work and supports the quality of the used models.

5 Acknowledgements

The authors acknowledges the funding of Grant Fondecyt 1180017 and the National Agency for Research and Development (ANID, Chile) for his PhD scholarship [ANID-PFCHA/Doctorado-Nacional/2019-21190164].

References

[1] Bünzli, J., *Trends in Chemistry*, **2019**, 1, 751-762.

[2] Bünzli, J., *Europ. J. of Inorg. Chem.*, **2017**, 44, 5058-5063.

[3] Bünzli, J., *J. of Lumines.*, **2016**, 170, 866-878.

[4] Jaztrzą, R., Nowak, M., Skrobańska, M., Tolińska, A., Zabiszak, M., Gabryel, M., Marciniak, L., Kaczmarek, M.T.,*Coord. Chem. Rev.*, **2019**, 382, 145-159.

[5] Ganjali, M., Gupta, V., Faridbod, F.Norouzi, P., *Elsevier*, **2016**.

[6] Ning, Y., Zhu, M., Zhang, J.L., *Coord. Chem. Rev.*, **2019**, 399, 213028.

[7] Khanagwal, J., Kumar, R., Devi, R., Bala, M., Sehrawat, P., Khatkar, S.P., Taxak, V.B., *Luminescence*, **2021**, 1-13.

[8] Kalyani, N.T.,Swart, H.,Dhoble, S.J., *Woodhead Publishing*, **2017**.

[9] Bao, G., *J. of Lumin.*, **2020**, 228, 117622.

[10] Georgieva, I., Trendafilova, N., Zahariev, T., Danchova, N., Gutzov, S., *J. of Luminescence*, **2018**, 202, 192-205.

[11] Ferreira da Rosa, P.P., Kitagawa, Y., Hasegawa, Y., *Coord. Chem. Rev.*, **2020**, 406, 213153.

[12] Parker, D., Fradgley, J.D., Wong, K.L., *Chem. Soc. Rev.*, **2021**,

[13] Weissman, S.I., *J. of Chem. Phys.*, **1942**, 10, 214-214.

[14] Moore, E.G., Samuel, A.P.S., Raymond, K.N., *Acc. Chem. Res.*, **2010**, 32, 736-740.

[15] Leonard J.P., Nolan C.B., Stomeo F., Gunnlaugsson T., *Top. in Current Chem.*, **2007**, 281, 1-43.

[16] Bünzli, J., *Coord. Chem. Rev.*, **2015**, 293-294, 19-47.

[17] Dasari, S., Singh, S., Sivakumar, S., Patra, A.K., *Chem. Eur. J.*, **2016**, 22, 17387-17396.

[18] Latva, M., Takalo, H., Mukkala, V.M.,Matachescu, C., Rodriguez-Ubis, J.C., Kankare, J., *Luminescence*, **1997**, 75,149-169.

[19] Bettencourt-Dias, A., Rossini, J.S.K., *Inorg. Chem.*, **2016**, 55, 9954-9963.

[20] Cockell, C.S., Knowland, J., *Biol. Rev.*, **1999**, 74, 311-345.

[21] Dinkova-Kostova, A.T., *Planta Med.*, **2008**, 74, 1548-1559.

[22] Sies, H., Stahl, W., *Photochem. Photobiol. Sci.*, **2004**, 3, 749-752.

[23] Chen, Z.F., Liu, Y.C., Huang, K.B., Liang, H., *Curr. Topics in Med. Chem.*, **2013**, 13, 2104-2115.

[24] Perez, D.R., Sklar, L.A., Chigaev, A.,*Pharm. and Therap.*, **2019**, 199, 155-163.

[25] Chen, Z.F., Song, X.Y., Peng, Y., Hong, Y., Liu, Y.C., Liang, H., *Dalton Trans.*, **2011**, 40, 1684-1692.

[26] Ding, W.Q., Liu, B., Vaught, J.L., Yamauchi, H., Lind, S.E., *Cancer Research*, **2005**, 65, 3389-3395.

[27] Yu, H., Zhou, Y., Lind, S.E., Ding, W.Q., *Biochem. J.*, **2009**, 417, 133-139.

[28] Jia, P., Ouyang, R., Cao, P., Tong, X., Zhou, X., Lei, T., Zhao, Y., Guo, N., Chang., H., Miao, Y., Zhou, S.,*J. of Coord. Chem.*, **2017**, 70, 2175-2201.

[29] Chen, Z.F., Gu, Y.Q., Song, X.Y., Liu Y.C., Peng, Y. Liang, *Eurp. J. of Med. Chem.*, **2013**, 59, 194-202.

[30] Chen, Z.F., Wei, J.H., Liu, Y.C., Liu M., Gu, Y.Q., Huang, K.B., Wang, M., Liang, H., *Europ. J. of Med. Chem.*, **2013**, 68, 454-462.

[31] Lischka, H., Nachtigallová, D., Aquino, A.J.A, Szalay, P.G., Plasser, F., Machado, F.B.C., Barbatti, M., *Chem. Rev.*, **2018**, 118, 7293-7361.

[32] Beltrán-Leiva, M.J., Solis-Céspedes, E., Páez-Hernández D., *Dalton Trans.*, **2020**, 48, 7444-7450.

[33] Townsend, J., Kirkland, J.K., Vogiatzis, K.D., *Elsevier*, **2019**.

[34] Abbas, Z., Dasari, S., Beltrán-Leiva, M.J., Cantero-López, P., Páez-Hernández D., Arratia-Pérez, R., Patra, A.K., *New J. of Chem.*, **2019**, 43, 15139-15152.

[35] Beltrán-Leiva, M.J., Cantero-López, P., Zúñiga, C., Bulhões-Figueira, A., Páez-Hernández, D., Arratia-Pérez, R., *Inorg. Chem.*, **2017**, 57, 9200-9208.

[36] Beltran-Leiva, M.J., Páez-Hernandez, D., Arratia-Pérez, R., *Inorg. Chem.* **2018**, 57, 5120-5132.

[37] Liu, Y.C., Wei, J.H., Chen, Z.F., Liu, M., Gu, Y.Q., Huang, K.B., Li, Z.Q., Liang, H., *Europ. J. of Med. Chem.*, **2013**, 69, 554-563.

[38] Baerends, E.J., Ziegler, T., Autschbach, J., Bashford, D., Bérces, A., Bickelhaupt, F.M., Bo, C., Boerrigter, P.M., Cavallo, L., Chong, D.P., et al., Amsterdam Density Functional, SCM., Theoretical Chemistry, Vrije University, Amsterdam Netherlands, **2012**, http//www.scm.com.

[39] van Lenthe, E., Baerends, E.J., Snijders, J.G., *J. Chem. Phys.*, **1993**, 99, 4597-4610.

[40] Wang, F., Hong, G., Li, L., *Chem. Phys. Lett.*, **2000**, 316, 318-323.

[41] Perdew, J.P., Yue, W., *Phys. Rev. B: Condens.*, **1986**, 33, 8800.

[42] Perdew, J.P., Burke, K., Ernzerhof, M., *Phys. Rev. Lett.*, **1996**, 77, 3865.

[43] Van Lenthe, E., Baerends, E.J.,*J. Comput. Chem.*, **2003**, 24, 1142-1156.

[44] Neese, F., The orca Program System, Wiley Interdiscip. Rev. Comput. Mol. Sci., **2012**, 2, 73-78.

[45] D. Ganyushin, F. Neese, *J. of Chem. Phys.* **2013**, 138, 104113.

[46] F. Neese, *J. Chem. Phys.* ,**2005**, 122, 034107

[47] Nesse, F., Wennmohs, F., Hansen, A., Becker, U., *J. Chem. Phys.*, **2009**, 130, 114108.

[48] Izsák, R., Nesse, F., *J. Chem. Phys.*, **2011**, 135, 144105.

[49] Yanai, T., Tew, D.P., Handy, N.C., *Chem. Phys. Lett.*, **2004**, 393, 51-57.

[50] Roos, B., Taylor, P.R., Sigbahm, P.E.M., *Chem. Phys.*, **1980**, 48, 157-173.

[51] Malmqvist, P.A., Roos, B.O., *Chem. Phys. Lett.*, **1989**, 155,189-194.

[52] C. Angeli, R. Cimiraglia and J. P. Malrieu,*J. Chem. Phys.*, **2002**, 117, 9138 9153.

[53] El-sayed, M.A., *J. of Chem. Phys.*, **1963**, 38, 2834-2838.

[54] El-sayed, M.A., *Acc. of Chem. Res.*, **1968**,1, 8-16.

[55] Penfold, T.J., Gindensperger, E., Daniel, C., Marian, C.M., *Chem. Rev.*, **2018**, 118, 6975-7025.

[56] Marian, C.M., *WIREs Comp. Mol. Sc.*, **2012**, 2, 187-203.

[57] Hess, B.A., Phys. Rev. A, **1986**, 33, 3742-3748.

[58] Pantazis, D.A., Neese, F., *J. Chem. Theory Comput.*, **2009**, 5, 2229-2238.

[59] A. Schäfer, H. Horn and R. Ahlrichs,*J. Chem. Phys.*, **1992**, 97, 2571 2577.

[60] K. Eichkorn, F. Weigend, O. Treutler and R. Ahlrichs, *Theor. Chem. Acc.*, **1997**, 97, 119 124.

[61] Weigend, F., Ahlrichs, R., *Chem. Phys.*, **2005**, 7, 3297-3305.

[62] Fetooh, H., Synthesis, *Egyp. J. of Chem.*, **2020**, 63, 1811-1822.

[63] Zhang, W.W., He, X.L., Deng, N., Wang, Y., He, J.B., *Electrochimica Acta*, **2014**, 127, 403-409.

[64] de Souza, B., Neese, F., Izsák, R., *J. of Chem. Phys.*, **2018**, 148, 034104.

[65] de Souza, B., Farias, G., Neese, F., Izsák, R., *J. of Chem. and Theo. Comp.*, **2019**, 15, 1896-1904.

[66] Gangan, T.V.U., Sreenadh, S., Reddy, M.L.P., *J. of Phot. and Photobi. A: Chemistry*, **2016**, 328, 171-181.

[67] Shuvaev, S., Utochnikova, V., Marciniak, Ł., Freidzon, A., Sinev, I., Deun, R.V., Freire, R.O., Zubavichus, Y., Grünert, W., Kuzmina, N., *Dalton Trans.*, **2014**, 43, 3121-3136.

[68] Biju, S., Freire, R.O., Eom, Y.K., Scopelliti, R., Bünzli, J.C.G., Kim, H.K., *Inorg. Chem.*, **2014**, 53, 8407-8417.

[69] Hardy, D.A., Tigaa, R.A., Ortega, R.E., McBride, J.R., Strouse, G.F., *J. Phys. Chem. C*, **2019**, 123, 31175-31182.

[70] Bozoklu, G., Marchal, C., Pécaut J., Imbert, D., Mazzanti, M., *Dalton Trans.*, **2010**, 39, 9112-9122.

[71] Tanner, P.A., Yeung, Y.Y., Ning, L., *J. of Phys. Chem. A*, **2013**, 117, 2771-2781.

[72] Guzmán-Méndez, O. González, F., Bernes, S., Flores-Álamo, M., Ordóñez-Hernández, J., García-Ortega, H., Guerrero, J., Qian, J., Aliaga-Alcalde, N., Gasque, L., *Inorg. Chem.*, **2018**, 57, 908-911.

[73] Cosby, A., Woods, J., Nawrocki, P., S∅rensen, Wilson, J.J., Boros, E., *Chem. Science*, **2021**, 12, 9442-9451.

[74] Zhang, Y., Thor, W., Wong, K.L., Tanner, P.A., *J. of Phys. Chem. C*, **2021**, 125, 7022-7033.